A micro-rheological and rheological study of biopolymers solutions: Hyaluronic acid

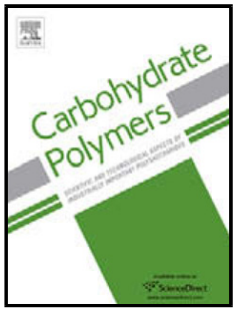

Title: A micro-rheological and rheological study of biopolymers solutions: Hyaluronic acid

Authors: Andrea Dodero, Rhodri Williams, Simona Gagliardi, Silvia Vicini, Marina Alloisio, Maila Castellano

PII: S0144-8617(18)31147-0
DOI: https://doi.org/10.1016/j.carbpol.2018.09.072
Reference: CARP 14115

To appear in:

Received date: 16-5-2018
Revised date: 5-9-2018
Accepted date: 27-9-2018

Please cite this article as: Dodero A, Williams R, Gagliardi S, Vicini S, Alloisio M, Castellano M, A micro-rheological and rheological study of biopolymers solutions: Hyaluronic acid, *Carbohydrate Polymers* (2018), https://doi.org/10.1016/j.carbpol.2018.09.072

A MICRO-RHEOLOGICAL AND RHEOLOGICAL STUDY OF BIOPOLYMERS SOLUTIONS: HYALURONIC ACID

Andrea Dodero[1], Rhodri Williams[2], Simona Gagliardi[3], Silvia Vicini[1], Marina Alloisio[1], Maila Castellano[1]*

[1]Università degli Studi di Genova, Dipartimento di Chimica e Chimica Industriale, Via Dodecaneso 31, 16146 Genova, Italy

[2]North Werber Road, Edinburgh EH4 1TA, UK

[3]Heriot Watt University, School of Engineering & Physical Sciences, Riccarton Campus, Edinburgh EH14 4AS, UK

* Corresponding author: Maila Castellano, maila.castellano@unige.it, +390103538706.

Chemical compound studied in this article:

Hyaluronic sodium salt (PubChem CID: 3084049), Sodium chloride (PubChem CID: 5234)

Highlights

- Hyaluronic acid used as injectable fillers containing nanoparticles or biomolecules
- Combination of Dynamic Light Scattering and traditional rotational rheometry
- Hydrodynamic radius and conformation of a polyelectrolyte in a saline environment
- Accessible frequency range significantly extended
- Parameters of the network created by the chain entanglements

ABSTRACT

Hyaluronic acid (HA) solutions represent an important class of biomedical products, mostly used as viscosupplements in orthopaedics and as fillers in the cosmetic industry. The focus of the present work

is the hydrodynamic, micro-rheological and rheological characterization of HA in physiological saline. Standard viscoelastic characterization techniques were coupled with micro-rheological measurements, i.e. by measuring the passive motions of particles embedded in the samples via Dynamic Light Scattering (DLS), effectively extending the accessible frequency range typical of standard rheometers. The influence of molecular weight and polymer concentration on the storage modulus (G'), loss modulus (G") and complex viscosity (η*) of HA saline solutions was investigated. A brief comparison with theoretical models was made showing such concentrated solutions to be of a semi-flexible nature. In addition, the entanglement concentration ν, the critical molecular weight $\bar{M}_c$, and the mesh size ξ of the physical network created by the entangled polymer chains were calculated.

Keywords: hyaluronic acid; dynamic light scattering; microrheology; rheology; mesh size.

1. Introduction

Hyaluronic acid (HA), a naturally occurring biopolymer (Freeman et al., 2015; Meyer & Palmer, 1934), shows very promising properties (biocompatibility, biodegradability and ease of functionalization), making it ideally suited for a number of clinical applications, e.g. supplementation of joint fluids, tissue engineering, eye surgery, wound healing, and drug delivery (Highley, Prestwich, & Burdick, 2016; Kogan, Soltés, Stern, & Gemeiner, 2007). HA is e a component of the extracellular matrix and exists as a high molecular weight glycosaminoglycan composed of disaccharide repeats of N-acetyl glucosamine and glucuronic acid (Fig. 1), linked together by an alternation of beta-1,4 and beta-1,3 glycosidic bonds (Chen & Abatangelo, 1999).

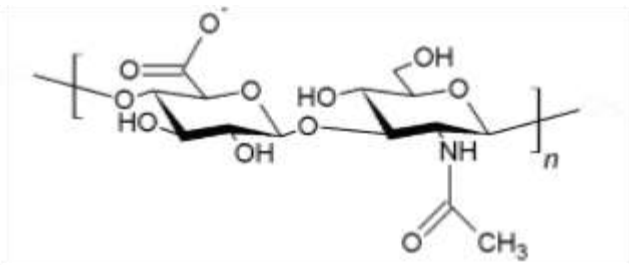

Fig. 1. Chemical structure of Hyaluronic Acid.

In solution, the backbone of HA is constricted by the synergy of the chemical structure of the molecule, internal hydrogen bonds, and interactions with the solvent, resulting in a twisting ribbon structure. Moreover, with HA being a polyelectrolyte (Cleland, Wang, & Detweiler, 1982), it behaves like a semi-rigid chain in water, while in a saline environment, the charges being screened, it takes on the form of an expanded random coil. Solutions of hyaluronic acid show very interesting rheological properties with a Newtonian behaviour at low-shear rates and a marked decrease in viscosity as the shear-rate increases; the polymer chains tend to entangle at low concentration, showing viscoelastic behaviour, i.e. while they act as viscous liquid at low frequency, they show elastic behaviour at higher frequency (Cowman & Matsuoka, 2005; Necas, Bartosikova, Brauner, & Kolar, 2008).

The aim of the present work is to carry out a detailed hydrodynamic and rheological characterization of HA solutions in physiological saline, in which both the molecular weight and concentration dependence were studied. For the hydrodynamic characterization, an approach based on dynamic light scattering (DLS), a non-destructive optical technique widely used to analyse the size distribution of a variety of systems (Berne & Pecora, 1977; Hassan, Rana, & Verma, 2015; Schartl, 2007), was utilised to verify the actual conformation adopted by HA chains in the studied environment. Alongside the regular DLS procedure, an innovative rheological methodology, DLS micro-rheology, was used to investigate the behaviour of HA solutions. Micro-rheology is a technique that evaluates the rheological properties of soft materials by measuring and analysing the displacement of probe particles (tracers) embedded in the sample (Chaikin & Lubensky, 2000; Dasgupta, Tee, Crocker, Frisken, & Weitz, 2002; Gardel, Valentine, Crocker, Bausch, & Weitz, 2003; Mason, 2000; Mason & Weitz, 1995). Rheological data obtained from DLS micro-rheology and those obtained from a conventional rotational rheometer were combined; this facilitated an extension of the frequency range over which the viscoelastic properties of HA solutions could be investigated (Squires & Mason, 2010). In addition, the possibility to use these systems as carriers for biomolecules (e.g. proteins, drugs, etc) and/or nano-objects (McHughs, DesNoyer, & Raman, 2006; Tan et al., 2009) was evaluated through parameters referring to network structure , i.e. ν, $\bar{M}_c$ and ξ, indicating the entanglement concentration, the average molecular weight

and the average distance between two entanglements, respectively (Canal & Peppas, 1989; Pesciolino et al., 2012).

2. Materials and Methods

2.1 *Materials*

Sodium hyaluronate with an average molecular weight of 90 kDa (HA_{90}), 1100 kDa (HA_{1100}), 1800 kDa (HA_{1800}), and 4000 kDa (HA_{4000}), was kingly provided by HTL Biotechnology (France) and produced by bacterial fermentation. Protein contents for the above samples ranged from < 0.01% to a maximum of 0.03%. Sodium chloride anhydrous ≥ 99.5% was purchased from Sigma-Aldrich. Polystyrene latex (PS) particles, diameter 1.0 μm, were purchased from micromod Partikeltechnologie GmbH (Rockstock, Germany). All the materials were used as provided without any further modification.

2.2 *HA solutions preparation*

HA was dissolved in physiological saline (0.15 M NaCl) under gentle stirring at room temperature for at least 48 hours until complete dissolution had occurred. Saline solution was filtered, before adding HA, using PTFE membrane syringe filters (pore size 0.2 μm). The solutions were then stored at 4 °C.

2.3 *DLS – Size and micro-rheological measurements*

In the current work, all DLS measurements, both size and micro-rheological, were performed using a Malvern Zetasizer Nano ZS (Malvern Instruments Ltd., UK), with a detection angle of 173° and a 4 mW He-Ne laser operating at a wavelength of 633 nm. At least 5 measurements on each sample were carried out to check for repeatability; temperature was set at 20 °C for all measurements.

DLS techniques make use of a coherent monochromatic light source and detection optics to determine the intensity fluctuations in the light scattered from the investigated sample. Information about the dynamics of the scatterers can be obtained by the normalized intensity autocorrelation function $g^{(2)}(q,\tau)$, given by:

$$g^{(2)}(q,\tau) = \frac{\langle I_S(\boldsymbol{q},0) I_S(\boldsymbol{q},\tau)\rangle}{\langle I_S(\boldsymbol{q},0)\rangle} \qquad (1)$$

where q is the scattering vector and τ the time delay (Grynkiewicz, Poenie, & Tsien, 1985). Using the Siegert relation (Voigt & Hess, 2002), the field autocorrelation function $g^{(1)}(q,\tau)$ is then obtained:

$$g^{(2)}(q,\tau) = 1 + \beta\left|g^{(1)}(q,\tau)\right|^2 \qquad (2)$$

where β represents the coherence factor and depends on the experimental set-up.

In DLS experiments, the field autocorrelation function decays with the diffusion coefficient D of the scatterers as follows:

$$g^{(1)}(q,\tau) = e^{-Dq^2r} \qquad (3)$$

According to the Stokes-Einstein relation, for a spherical object, D can be expressed as:

$$D = \frac{k_B T}{6\pi\eta R_H} \qquad (4)$$

where k_B is the Boltzmann's constant, T the temperature, η the viscosity of the solvent and R_H the scatterers hydrodynamic radius (Berne & Pecora, 1977).

In DLS micro-rheology, micron sized spherical tracer particles are embedded in the material and their motion, due to thermal energy, is measured. In case of a three dimensional random walk, D can be correlated to the mean square displacement (MSD) of the tracers $\langle\Delta r^2(\tau)\rangle$:

$$D = \frac{\langle\Delta r^2(\tau)\rangle}{6\tau} \qquad (5)$$

Combining this with equation (3), it is possible to calculate $\langle\Delta r^2(\tau)\rangle$ inverting the field autocorrelation function. If the tracers are embedded in a viscoelastic medium, the rheological properties can be obtained using the Generalized Stokes-Einstein Relation (GSER):

$$\tilde{G}(s) = \frac{k_B T}{\pi a s\langle\tilde{r}^2(s)\rangle} \qquad (6)$$

where $\langle\tilde{r}^2(s)\rangle$ represents the Laplace transform of the MSD and $\tilde{G}(s)$ is the viscoelatic spectrum as a function of s, the Laplace frequency (Kholodenko & Douglas, 1995). From equation (6), using the numerical method of Mason and Weitz (Mason & Weitz, 1995) it is possible to calculate the storage

and loss modulus. Briefly, fitting the MSD plot to a power law and calculating the logarithmic differential, an algebric form of GSER is obtained:

$$|G^*(\omega)| \approx \frac{k_B T}{\pi a \langle \Delta r^2(\tau=\frac{1}{\omega}) \rangle \Gamma\left[1+\alpha(\tau=\frac{1}{\omega})\right]} \qquad (7)$$

where Γ is the gamma function.

Finally, the storage and loss moduli can be obtained:

$$G'(\omega) = |G^*(\omega)| \cos(\delta(\omega)) \qquad (8)$$

$$G''(\omega) = |G^*(\omega)| \sin(\delta(\omega)) \qquad (9)$$

where δ(ω) is defined as:

$$\delta(\omega) = \frac{\pi}{2} \frac{d ln\, |G^*(\omega)|}{d ln\, \omega} \qquad (10)$$

In the current work, a characterization of all available HA samples was performed in physiological saline in order to investigate the hydrodynamic radius R_H and the effective conformation of the polymer chains (La Gatta, De Rosa, Marzaioloi, Busico, & Schiraldi, 2010). For each $\bar{M}_W$, solutions with decreasing concentration were tested until R_H assumed a constant value, to ensure no aggregates were present. For HA, a refractive index of 1.563 and an absorption value of 0.001 were used (Tadmor, Chen, & Israelachvili, 2002). For physiological saline, a viscosity of 1.02 mPa·s and a refractive index of 1.332 were utilised (Biradar & Dongarge, 2015).

The micro-rheological characterization of HA in physiological saline hereby described was performed on solutions of HA_{1100}, HA_{1800} and HA_{4000}. The provided 50 mg/mL PS particle suspension was diluted to 0.01 mg/mL, using physiological saline, and then used to prepare all samples for micro-rheological measurements. For the tracers, a refractive index of 1.59 and an absorption of 0.01 were used (Ma et al., 2013). In order to obtain reliable micro-rheological data, certain conditions about the tracer-sample combination must be verified. A first pre-measurement step was used to assess the suitability of PS particles by measuring the zeta potential (ζ) of the tracers in the dispersant only and then in the presence of the sample; the difference between the two values, ideally < 5 mV, gives information about the tracer-

sample interactions, which should be minimal. As reported in literature (Hnyluchóva, Mondek, & Pekar, 2014), the concentration of the sample does not influence these interactions; therefore for each $\bar{M}_W$ only a single HA saline solution with a concentration of 1 mg/mL was tested. A second pre-measurement step was used to predict the tracer concentration required to give a relative intensity ratio of 95%; in the present case, 10 μL of the 0.01 mg/mL tracer suspension were added to 2 mL of HA solutions. The mixtures were placed into a rotating mixer for a minimum of 48h to ensure homogeneous dispersion of PS particles within the solutions and subsequently tested.

The required hydrodynamic radius of the tracers (De Smedt et al., 1994) of the PS particles was measured in physiological saline at a concentration of 0.01 mg/mL; a value of 1.1 μm was obtained, which is consistent with the given nominal size of 1.0 μm. This result confirmed that PS particles do not aggregate in the used environment, which is extremely important in order to obtain reliable data from the micro-rheological characterization.

On the basis of the results, HA solutions in physiological saline were prepared adding the required PS particles and micro-rheological tests were performed to evaluate the viscoelastic properties.

2.4 *Rheological measurements*

Rheological measurements were performed using an AR-G2 rotational rheometer (TA Instruments, USA), equipped with a Peltier heating system. At least 3 measurements at 20 °C on each sample were carried out to check for repeatability. The HA solutions tested were the same tested with DLS microrheology.

The measurements were carried out using a 60 mm cone/plate geometry, 1° cone angle and 58 μm truncation. On each sample, an amplitude sweep test was performed to determine the linear viscoelastic region (LVER) at a fixed frequency of 1 Hz and a strain (γ) varying from 0.1 to 75%. Subsequently, frequency sweep tests were carried out varying the frequency from 0.01 to 40 Hz, at a deformation within the LVER.

3. Results and Discussion

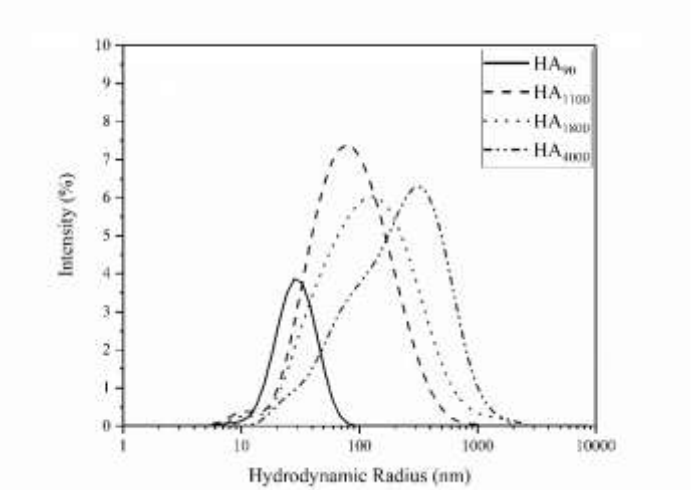

Fig. 2. Distribution functions of the hydrodynamic radius obtained for HA ~~solutions~~ at 20 °C in 0.15 M NaCl.

3.1 *Hydrodynamic Radius, conformation and critical overlap concentration c**

Figure 2 shows the HA size distributions obtained from DLS size measurements. The plot reports the relative percentage of light scattered by HA molecules as a function of the calculated R_H.

HA_{90}, HA_{1100} and HA_{1800} show a monomodal distribution, indicating that aggregates are not present; conversely, HA_{4000} shows a bimodal distribution, suggesting the presence of a significant fraction of polymer at a lower molecular weight. All the tested samples appear to be significantly polydispersed, HA being a natural polymer. However, to be noted that R_H corresponds to the radius of a sphere that moves according to thermal motions; if a layer of solvent surrounds the molecules during their diffusion, the characterization may be affected (Nelson & Cosgrove, 2004) and consequently the samples may show high polydispersity in terms of R_H. As expected, the results show an increasing R_H with increasing $\bar{M}_W$.

In order to check the effective conformation of HA in physiological saline, the molecular weight $\bar{M}_W$ was related to the molecular size R_g (Shimamura & Deguchi, 2001), which was obtained from R_H by the well-known relationship for spheroidal objects (Kok & Rudin, 1981; Smilgies & Folta-Stogniew, 2015), reported in equation (11):

$$R_g = 0.775 R_H \qquad (11)$$

The results are summarized in Table 1.

From equation (12):

$$R_g \sim \bar{M}_W{}^{a} \qquad (12)$$

it is possible to obtain the Flory exponent a, which gives information about the conformation of the macromolecules; a = 1 suggests that the polymer molecules are rigid rods, a value between 0.5 and 0.67 is associated to random coils, and a value of 0.3 occurs for spheres (Mendichi, Soltés, & Schieroni, 2003; Pollock, Ashton, Rode, Schaffer, & Healy, 2012; Smilgies & Folta-Stogniew, 2015). Figure 3 shows the experimental R_g vs. $\bar{M}_W$ giving an experimental value of 0.556.

The obtained value indicates a random coil conformation for HA in physiliogical conditions ; indeed, in this environment the negative charges on the chains are shielded by the ions in solution. Conversely,

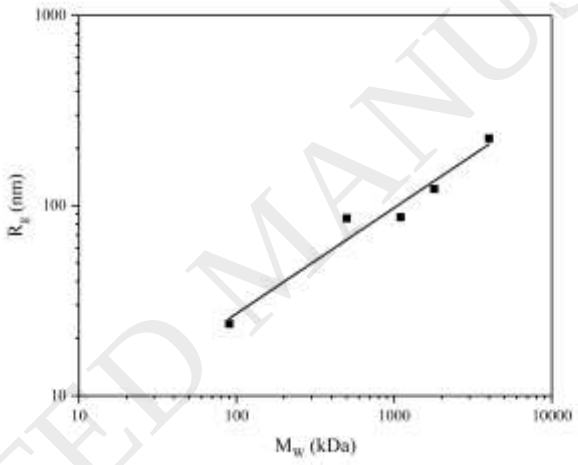

Fig. 3. Relationship between the gyration radius and the molecular weight of HA.

in water, the charges tend to repel each other, and the polymer behaves as a semi-rigid extended chain (Podzimek, Hermannova, Bilerova, Bezakova, & Velebny, 2010). As reported in literature (Horkay, Basser, Londono, Hecht, & Geissler, 2009; Kim, Woo, Park, Hwang, & Moon, 2015), the used salt concentration (0.15 M NaCl) is significantly higher than the shielding concentration, which was further confirmed by the obtained random coil conformation (see Fig. 3).

The concentration at which the polymer chains start to overlap, known as critical overlap concentration c* (Larson, 1999; Rao, 2007), can be calculated by:

$$c^* = \frac{\bar{M}_W}{R_g^3 A} \qquad (13)$$

where A is Avogadro's number.

Table 1 reports the obtained results for the different $\bar{M}_W$ tested along with their hydrodynamic radius R_H, the polydispersion index d (obtained by size exclusion chromatography with refractive index and light scattering detectors), and the radius of gyration R_g.

The data show that c* decreases with increasing molecular weight. As expected, the higher the $\bar{M}_W$, the longer the polymer chains; thus they tend to overlap at a lower concentration.

3.2 *Tracers dimension, compatibility and concentration*

In physiological saline, the used PS particles showed a hydrodynamic radius of 1.1 μm; this value is much larger than the average hyaluronan mesh size found in literature (Horkay, Basser, Hecht, & Geisser, 2013; Shenoy, Rosenblatt, Vincent, & Gaigalas, 1995). Under this condition, the tracers investigate the bulk properties of HA solutions and the assumption of continuum viscoelasticity can be assumed valid.

The difference in terms of potential, between the tracers/dispersant (ζ_A) and the tracers/HA (ζ_B), obtained by measuring the two zeta potentials, was lower than the acceptable zeta ratio (5 mV) for all samples, indicating that interactions between hyaluronic acid and polystyrene particles (tracers) do not occur (Hnyluchovà et al., 2014).

For the minimum tracer concentration required, the results were obtained testing the relative intensity of tracer particles scattering against sample matrix. The intensity of the scattering from the particles must be higher than the intensity of the scattering from HA and, as expected, the results show that for a given molecular weight, the minimum tracers concentration required increases with HA concentration.

3.3 *Rheological properties*

The rheological behaviour of HA solutions was studied both on a standard rheometer and via DLS, extending the frequency range of investigation. Particular attention was paid to the elastic (or storage) modulus, G', the viscous (or loss) modulus, G", indicating the capability of materials to store and dissipate energy, and to the complex viscosity, η*, representing the total resistance to flow.

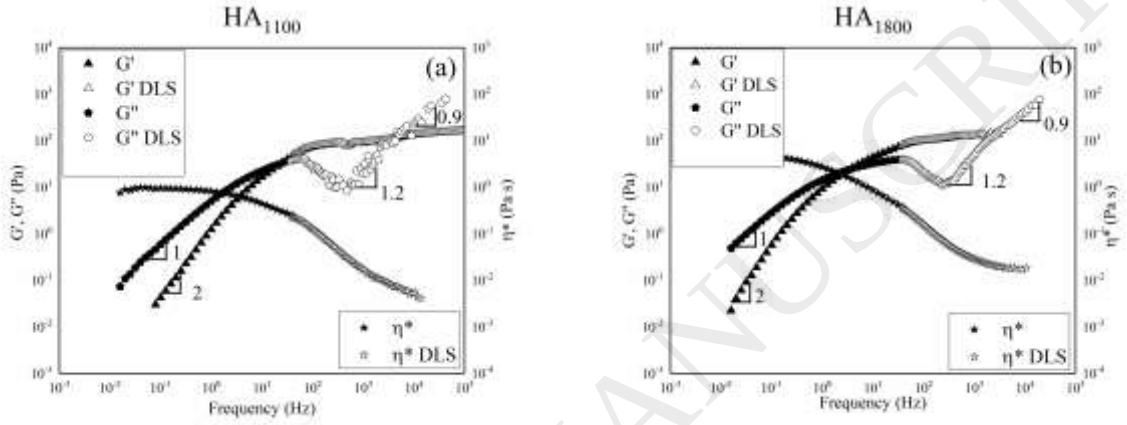

Fig. 4. Average storage G', loss modulus G" and complex viscosity η* superimposed for 10 mg/mL solution of a) HA_{1100}; b) HA_{1800}.

A typical result for the frequency dependence of the viscoelastic moduli and the complex viscosity is presented in Fig. 4 for HA solutions with a concentration of 10 mg/mL and different molecular weight. Here data from standard rheological measurements are shown to perfectly overlap to the extended range provided by DLS measurements for all the $\bar{M}_W$ investigated.

All the tested samples show the typical behaviour of polymer solutions. Particularly, at low frequencies the loss modulus G" dominates, indicating the samples mostly behave like a liquid; the first crossover between G' and G" indicates the point where the samples start to show a solid-like behaviour, with the storage modulus becoming almost constant while G" decreases with increasing frequency. The second crossover indicates the point where the samples undergo a phase transition , with G" increasing significantly. This rheological behaviour is typical of polymer chains above the entanglements concentration c_e, where chains entangle and form a transient network (De Smedt, Dekeyser, Ribitisch, Lauwers, & Demeester, 1993; Gribbon, Heng, & Hardingham, 1999; Kobayashi, Okamoto, &

Nishinari, 1994). At low frequencies (long timescales), these chains have sufficient time to disentangle and the behaviour is that of a viscous liquid, while at intermediate frequencies the polymer chains cannot free themselves from the entanglements within the shorter timescale, therefore acting as an elastic network and leading to an elastic plateau region, called rubbery plateau region (Doi & Edwards, 1986). At higher frequencies, corresponding to very short timescales, HA solutions are subjected to a phase transition ; in this region, the polymer chains start to lose their mobility, except for localized modes of deformation (Leibler, Pezron, & Pincus, 1988). Further increasing the frequencies, a third crossover between the viscoelastic moduli can be observed (not reached with our experiments); in this terminal region, the polymer is characterized by a glassy behaviour, with the chains completely immobilized and where G' is higher than G".

As expected, the viscoelastic properties of HA solutions are strongly influenced by the molecular weight ; for a fixed HA concentration, increasing $\bar{M}_W$ corresponds to higher values of G', G" and η* since longer chains lead to a higher amount of entanglements present in the system, as reported in Table 2. Moreover, the first crossover frequency, at which the rubbery behaviour becomes predominant, tends to decrease with increasing the molecular weight , corresponding to longer time necessary for the polymer chains to disentangle.

The low frequency dependency of the moduli is found to be proportional to ω^2 and ω^1 for G' and G'' respectively, as expected (Colby, 2009). At intermediate frequency the plateau reached by G' was used to calculate the network parameters (see below). At higher frequencies, where adequate, slopes were calculated for G" (see Fig. 4) and found to be around 1.2, then decreasing to 0.8-0.9, irrespectively of $\bar{M}_W$ and concentration. Nevertheless HA is itself a semi-rigid charged biopolymer, made flexible by the screening of the charges (0.15 M NaCl) and assuming an expanded random coil conformation (Buhler & Boué, 2003), the obtained result would indicate, according to Morse (Morse, 1998), HA to behave more as a semiflexible rod-like polymer tightly entangled (slope 1 then decreasing to 0.75 at very high frequency, outwith our range). This is not entirely surprising because the high frequency data provides an insight into more localised motions, where the intrinsic stiffness of the HA chains seems to still maintain a role.

The concentration dependence of the viscoelastic properties for a given molecular weight was also studied; the frequency dependence of G' and η* for different concentrations of HA_{1800} solutions is shown in Fig. 5 (a) and (b) respectively.

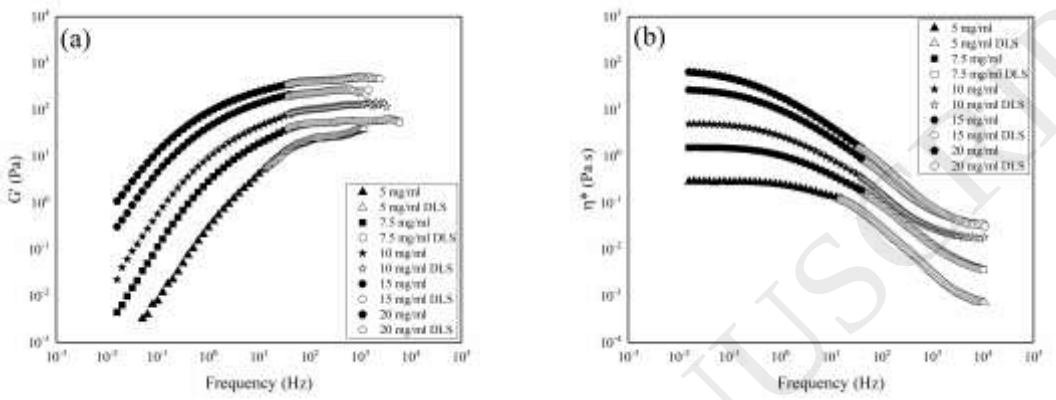

Fig. 5. a) Storage modulus G'; b) Complex viscosity η* for 5, 7.5, 10, 15, 20 mg/mL HA_{1800} solutions.

As expected, the data show that both G' and η* increase with increasing HA concentration. In addition, a decrease of the frequency at which the rubbery plateau starts is noted for higher concentration. This behaviour is related to the fact that the higher the polymer concentration, the higher the amount of entanglements present in solution; consequently, samples show increased viscoelastic properties and a dominant elastic behaviour.

All tested HA solutions show a non-Newtonian shear-thinning behaviour (Sundaram, Voigts, Beer, & Melands, 2010; Zhong, Oostrom, Truex, Vermeul, & Szecsody, 2013); hereby dynamic data can be interconverted to viscosity (shear-rate) data, where Cox-Merz rule successfully applies (data not shown, manuscript in preparation). They are characterized by a high complex viscosity at low frequencies, which tends to show a several orders of magnitude decrease with increasing frequency, i.e. shear-thinning. This behaviour makes HA solutions suitable to the challenges of obtaining injectable polymer solutions, called fillers; a high viscosity helps fillers to remain in the right position once they are injected, while a low viscosity during the high shear injection process helps both to use concentrated systems and to reduce the pain (Guvendiren, Lu, & Burdick, 2012).

Table 2 summarizes the obtained values of G_0 (corresponding at G' in the rubbery plateau region, approximately taken at a frequency of 500 Hz; at this frequency, all the tested samples show to be in the elastic region), η_0^* and η_∞^* for the tested solutions. The values of η_0^* (complex viscosity extrapolated at zero shear rate) were taken in the Newtonian region (approximately 0.02 Hz), while the values of η^*_∞ at 10000 Hz.

3.4 *Network parameters*

The values of G_0 were used to calculate the parameters of the network structure, i.e. ν, $\bar{M}_c$ and ξ; ν represents the concentration of the entanglements (mol/vol), $\bar{M}_c$ the average molecular weight between two entanglements (solutions) or crosslinking points (hydrogels), and ξ the average distance between two entanglements (solutions) or crosslinking points (hydrogels), also known as mesh size (De Smedt et al., 1993). Being G_0 related to the amount of entanglements (Borzacchiello, Russo, Malle, Schwach-Abdellaoiu, & Ambrosio, 2015; D'Errico et al., 2008), it can be expressed as following:

$$G_0 = R \cdot T \cdot \nu \qquad (14)$$

where RT represents the thermal energy. ν can be calculated by:

$$\nu = \frac{G_0}{R \cdot T} \qquad (15)$$

or expressed as:

$$\nu = \frac{c}{\bar{M}_c} \qquad (16)$$

where c indicates the polymer concentration. By combining equation 14 and equation 16, it is possible to calculate $\bar{M}_c$ as follows:

$$\bar{M}_c = \frac{R \cdot T \cdot c}{G_0} \qquad (17)$$

Equation 17 must be corrected considering that the polymer chain end-segments, i.e. the dangling ends connected to the network by only one link, cannot store elastic energy and consequently they do not contribute to the elastic modulus. Equation 17 then becomes:

$$\bar{M}_c = \frac{R \cdot T \cdot c \cdot \bar{M}_n}{G_0 \cdot \bar{M}_n + 2R \cdot T \cdot c} \qquad (18)$$

(Borzacchiello et al., 2015; Flory, 1953) with $\bar{M}_n$ representing the number average molecular weight of the polymer, calculated by $\bar{M}_W$ and the polydispersity index. Considering the equivalent network model (Schurz, 1991), it is possible to calculate the mesh size ξ as:

$$\xi = \sqrt[3]{\frac{6\bar{M}_c}{\pi \cdot c \cdot A}} \qquad (19)$$

Table 2 summarizes the results obtained for HA solutions using equations 15, 18 and 19.

Fixing $\bar{M}_W$, the highest values of $\bar{M}_c$ and ξ were found for the sample with the lowest starting concentration, corresponding to the lowest concentration of entanglements ν. On the contrary, the sample with the highest starting concentration shows the lowest values of $\bar{M}_c$ and ξ, corresponding to the highest concentration of entanglements ν. Moreover, HA concentration, the network parameters decrease with increasing the molecular weight; indeed, the higher the $\bar{M}_W$ the more the sample is entangled. Knowing the mesh size of the physical network formed by HA chains in solution could lead to the use of these systems as carriers of biomolecules with an appropriate dimension, such as insulin and/or other proteins.

Figure 6 reports the concentration dependence of G_0 for the different molecular weights tested. The plateau modulus G_0 increases with increasing polymer concentration according to a power law behaviour $G_0 \sim c^{\alpha}$; in all cases, α lies in the range from 2.0 (HA_{1800}) to 3.0 (HA_{1100}, HA_{4000}). These values are in good agreement with the theoretical value for entangled network of semiflexible chains (MacKintosh, Käs, & Janmey, 1995; Schuldt et al., 2016; Tassieri, Evans, Warren, Bailey, & Cooper, 2012).

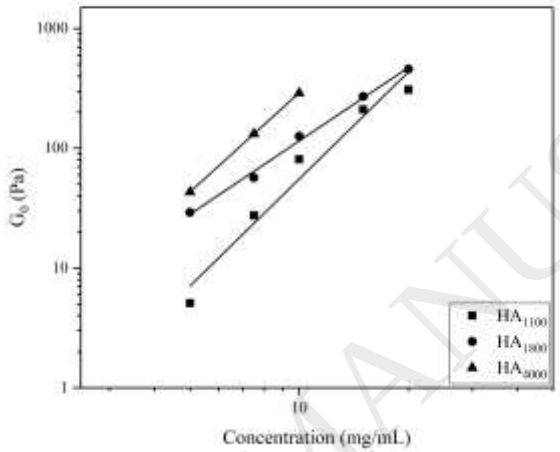

Fig. 6. Dependence of the plateau modulus G_0 on ~~the~~ polymer concentration.

4. Conclusion

The obtained results demonstrated that DLS is a powerful technique that allows the study of both hydrodynamic and rheological behaviour of polymer solutions.

HA chains behave as random coils in physiological saline, due to the screening of the negative charges present on the polymer backbone by the ions in solution. We found that the hydrodynamic radius R_H increases with increasing the molecular weight; contrariwise, the overlap concentration c* decreases with increasing $\bar{M}_W$, indicating that bigger coils start to overlap with each other at lower polymer concentration.

The combinated use of DLS Micro-rheology and traditional rheometry has shown that the two techniques are complementary; DLS Micro-rheological data, related to the high frequencies, perfectly

overlapped with the rheological data obtained from conventional measurements and related to the low frequencies. Therefore, we managed to significantly extend the frequency range in which was possible to investigate the viscoelastic behaviour of the studied systems (0.01-10000 Hz).

HA solutions show a liquid-like behaviour at low frequencies and a gel-like behaviour at high frequencies; in particular, with increasing both $\bar{M}_W$ and concentration, HA solutions show higher moduli and complex viscosity, combined with a marked shear-thinning behaviour. The latter one is much important since, even at high molecular weight and concentration, it allows the successful use of these systems as injectable fillers.

Interestingly, the calculated values of the mesh size ξ indicate that biomolecules and/or nanoparticles, with an appropriate dimension in the range of 200-600 nm, could be trapped in the physical network created by the entanglements and transported in the human body for a possible therapeutic effect.

Acknowledgement

The authors would like to thank Erasmus+ project for the support and HTL Biotechnology for having kindly provided the hyaluronic acid.

References

Berne, J. B., & Pecora, R. (1977). Dynamic light scattering: with application to chemistry, biology and physics. *Journal of Chemical Education, 54,* A430.

Biradar, V. U., & Dongarge, M. S. (2015). Refractive index of salt (NaCl) from aqueous solution. *International journal of computer & mathematical sciences, 4.*

Borzacchiello, A., Russo, L., Malle, B. M., Schwach-Abdellaoiu, K., &Ambrosio, L. (2015). Hyaluronic acid based hydrogels for regenerative medicine applications. *BioMed Rresearch International, 2015.*

Buhler, E., & Boué, F. (2003). Persistence length for a model semirigid polyelectrolyte as seen by small angle neutron scattering: a relevant variation of the lower bound with ionic strength. *The European Physical Journal E, 10,* 89-92.

Canal, T., & Peppas, A. N. (1989). Correlation between mesh size and equilibrium degree of swelling of polymeric networks. *Journal of biomedical materials research, 23,* 1183-1193.

Chaikin, M. P., & Lubensky, C. T. (2000). *Principles of condensed matter physics*. Cambridge: Cambridge University Press.

Chen, W. Y. J., & Abatangelo, G. (1999). Functions of hyaluronan in wound repair. *Wound repair and regeneration, 7,* 79-89.

Cleland, L. R., Wang, L. J., & Detweiler, M. D. (1982). Polyelectrolyte properties of sodium hyaluronate. *Macromolecules, 15,* 386-395.

Colby, R. H. (2009). Structure and linear viscoelasticity of flexible polymer solutions: comparison of polyelectrolyte and neutral polymer solutions. *Rheological Acta, 49,* 425-442.

Cowman, M. K., & Matsuoka, S. (2005). Experimental approaches to hyaluronan structure. *Carbohydrate research, 340,* 791-809.

D'Errico, G., De Lellis, M., Mangiapia, G., Tedeschi, A., Ortona, O., Fusco, S., Borzacchiello, A., & Ambrosio, L. (2008). Structural and mechanical properties of UV-photo-cross-linked poly(N-vinyl-2-pyrrolidone) hydrogels. *Biomacromolecules, 9,* 231-240.

Dasgupta, R. B., Tee, Y. S., Crocker, C. J., Frisken, J. B., & Weitz, A. D. (2002). Microrheology of polyethylene oxide using diffusing wave spectroscopy and single scattering. *Physical Review Letters, 65.*

De Smedt, S. C., Dekeyser, P., Ribitsch, V., Lauwers, A., & Demeester, J. (1993). Viscoelastic and transient network properties of hyaluronic acid as a function of the concentration. *Biorheology, 30,* 31-41.

De Smedt, S. C., Lauwers, A., Demeester, J., Engelborghs, Y., De Mey, G., & Du, M. (1994). Structural information on hyaluronic acid solutions as studied by probe diffusion experiments. *Macromolecules, 27,* 141-146.

Doi, M., & Edwards, S. F. (1988). *The theory of polymer dynamics.* Oxford: Oxford University Press.

Flory, P. J. (1953). *Principles of polymer chemistry.* Ithaca: Cornell University Press.

Freeman, R., Boekhoven, J., Dickerson, M. B., Naik, R. R., & Stupp, S. I. (2015). Biopolymers and supramolecular polymers as biomaterials for biomedical applications. *MRS bull, 40,* 1089-1101.

Gardel, L. M., Valentine, T. M., Crocker, C. J., Bausch, R. A., & Weitz, A. D. (2003). Microrheology of entangled F-actin solutions. *Physical Review Letters, 91.*

Gribbon, P., Heng, B. C., & Hardingham, T. E. (1999). The molecular basis of the solution properties of hyaluronan investigated by confocal fluorescence recovery after photobleaching. *Biophysical Journal, 77,* 2210-2216.

Grynkiewicz, G., Poenie, M., & Tsien, R. Y. (1985). A new generation of Ca2+ indicators with greatly improved fluorescence properties. *Journal of Biological Chemistry, 260,* 3440-3450.

Guvendire, M., Lu, H. D., & Burdick, J. A. (2012). Shear-thinning hydrogels for biomedical applications. *Soft Matter, 8,* 260.

Hassan, A. P., Rana, S., & Verma, G. (2015). Making sense of Brownian motion: colloid characterization by dynamic light scattering. *Langmuir, 31,* 3-12.

Highley, C. B., Prestwich, G., & Burdick, J. A. (2016). Recent advances in hyaluronic acid hydrogels for biomedical applications. *Current opinion in biotechnology, 40,* 35-40.

Hnyluchóva, Z., Mondek, J., Pekar, M. (2014). DLS microrheology of biopolymer solution, probe surface effect.

Horkay, F., Basser, P. J., Hecht, A., & Geisser, E. (2013). Structure and interactions in hyaluronic acid solutions. *Polymeric materials: science & engineering, 108,* 111-112.

Horkay, F., Basser, P. J., Londono, D. J., Hecht, A., & Geissler, A. (2009). Ions in hyaluronic acid solutions. *The Journal of Chemical Physics, 131*.

Kholodenko, A. L., & Douglas, J. F. (1995). Generalized Stoked Einsten equation for spherical particle suspension. *Physical Review E, 51,* 1081.

Kim, B., Woo, S., Park, Y., Hwang, E., & Moon, M. H. (2015). Ionic strength effect on molecular structure of hyaluronic acid investigated by flow field-flow fractionation and multiangle light scattering. *Analytical and Bioanalytical Chemistry, 407,* 1327-1334.

Kobayashi, Y., Okamoto, A., & Nishinari, K. (1994). Viscoelasticity of hyaluronic acid with different molecular weights. *Biorheology, 31,* 235-244.

Kogan, G., Soltès, L., Stern, R., & Gemeiner, P. (2007). Hyaluronic acid: a natural biopolymer with a broad range of biomedical and industrial applications. *Biotechnology letters, 29,* 17-25.

Kok, C. M., & Rudin, A. (1981). Relationship between the hydrodynamic radius and the radius of gyration of a polymer in solution. *Macromolecular rapid communications, 2,* 655-659.

La Gatta, A., De Rosa, M., Marzaioli, I., Busico, T., & Schiraldi, C. (2010). A complete hyaluronan hydrodynamic characterization using a size exclusion chromatography-triple detector array system during in vitro enzymatic degradation. *Analytical biochemistry, 404,* 21-29.

Larson, R. G. (1999). The structure and rheology of complex fluids. *Oxford university press.*

Leibler, L., Pezron, E., & Pincus, P. A. (1988). Viscosity behaviour of polymer solutions in the presence of complexing ions. *Polymer, 29,* 1105-1109.

Ma, X., Lu, J. Q., Brock, R. S., Jacobs, M. K., Yang, P., & Hu, X. (2003). Determination of complex refractive index of polystyrene microspheres from 370 to 1620 nm. *Physics in medicine & biology*, *48*, 4165-4172.

MacKintosh, F. C., Käs, J., & Janmey, P. A. (1995). Elasticity of Semiflexible Biopolymer Networks. *Physical Review Letters*, *75*, 4425.

Mason, G. T. (2000). Estimating the viscoelastic moduli of complex fluids using the generalized Stokes-Einstein equation. *Rheology acta*, *39*, 371-378.

Mason, G. T., & Weitz, A. D. (1995). Optical measurements of frequency-dependent linear viscoelastic moduli of complex fluids. *Physical review letters*, *74*, 1250-1253.

McHughs, J. A., DesNoyer, R. J., & Raman, C. (2006). *Polymeric drug delivery II*.

Mendichi, R., Soltés, L., & Schieroni, A. G. (2003). Evaluation of Radius of Gyration and Intrinsic Viscosity Molas Mass Dependence and Stiffness of Hyaluronan. *Biomacromolecules*, *4*, 1805-1810.

Meyer, K., & Palmer, J. W. (1934). The polysaccharide of vitreous humor. *Journal of biology and chemistry*, *107*, 629-634.

Morse, D. C. (1998). Viscoelasticity of concentrated isotropic solutions of semiflexible polymers. 2. Linear response. *Macromolecules*, *31*, 7044-7067.

Necas, J., Bartosikova, L., Brauner, P., & Kolar, J. (2008). Hyaluronic acid (hyaluronan): a review. *Veterinarni medicina*, *53*, 397-411.

Nelson, A., & Cosgrove, T. (2004). Dynamic light scattering studies of poly(ethylene oxide) adsorbed on laponite: layer conformation and its effect on particle stability. *Langmuir*, *20*, 10382-10388.

Pesciolino, L., Feruglio, L., Farra, R., Fiorentino, S., Colombo, I., Coviello, T., Matricardi, P., Hennink, E. W., Vermonden, T., & Grassi, M. (2012). Mesh size distribution determination of interpenetrating polymer network hydrogels. *Soft matter*, *8*, 7708-7715.

Podzimek, S., Hermannova, M., Bilerova, H., Bezakova, Z., & Velebny, V. (2010). Solution properties of hyaluronic acid and comparison of SEC-MALS-VIS data with off-line capillary viscometry, *Journal of applied polymer science, 116,* 3013-3020.

Pollock, J. E., Ashton, R. S., Rode, N. A., Schaffer, D. V., & Healy, K. E. (2012). Molecular characterization of multivalent bioconjugates by size-exclusion chromatography with multiangle laser light scattering. *Bioconjugate chemistry, 23,* 1794-1801.

Rao, M. A. (2007). *Rheology of fluid and semisolid foods principles and applications.* New York: Springer US.

Schartl, W. (2007). *Light scattering from polymer solutions and nanoparticles dispersion.* Berlin: Springer-Verlag Berlin Heidelberg.

Schuldt, C., Schnaub, J., Händler, T., Glaser, M., Lorenz, J., Golde, T., Käs, J. A., & Smith, D. M. (2016). Tuning Synthetic Semiflexible Networks by Bending Stiffness. *Physical Review Letters, 117*.

Schurz, J. (1991). Rheology of polymer solutions of the network type. *Progress in polymer science, 16,* 1-53.

Shenoy, V., Rosenblatt, J., Vincent, J., & Gaigalas, A. (1995). Measurement of mesh sizes in concentrated rigid and flexible polyelectrolyte solutions by an electron spin resonance technique. *Macromolecules, 28,* 525-530.

Shimamura, M. K., & Deguchi, T. (2001). Gyration radius of a circular polymer under a topological constraint with excluded volume. *Physical review E, 64.*

Smilgies, D., & Folta-Stogniew, E. (2015). Molecular weight-gyration radius relation of globular proteins: a comparison of light scattering, small-angle X-ray scattering and structure-based data. *Journal of applied crystallography, 48,* 1604-1606.

Squires, M. T., & Mason, G. T. (2010). Fluid mechanics of microrheology. *Annual review of fluid mechanics, 42,* 413-438.

Sundaram, H., Voigts, B., Beer, K., & Melands, M. (2010). Comparison of the rheological properties of viscosity and elastic in two categories of soft tissue fillers: calcium hydroxylapatite and hyaluronic acid. *Dermatological surgery, 36,* 1859-1865.

Tadmor, R., Chen, N., & Israelachvili, N. J. (2002). Thin film rheology and lubricity of hyaluronic acid solutions at a normal physiological concentration. *Journal of biomedical materials research, 61,* 514-523.

Tan, H., Ramirez, M. C., Miljkovic, N., Li, H., Rubin, P. J., & Marra, G. K. (2009). Thermosensitive injectable hyaluronic acid hydrogel for adipose tissue engineering. *Biomaterials, 30,* 6844-6853.

Tassieri, M., Evans, R. M. L., Warren, R. L., Bailey, N. J., & Cooper, J. M. (2012). Microrheology with optical tweezers: data analysis. *New Journal of Physics, 14.*

Voigt, H., & Hess, S. (2002). Comparison of the intensity correlation function and the intermediate scattering function of fluids: a molecular dynamics study of the Siegert relation. *Physica A: Statistical Mechanics and its Application, 202,* 145-164.

Zhong, L., Oostrom, M., Truex, M. J., Vermeul, V. R., & Szecsody, J. E. (2013). Rheological behaviour of xantham gum solution related to shear thinning fluid delivery for subsurface remediation. *Journal of hazardous materials, 244-245,* 160-170.

Table 1. Relevant obtained data for HA .

$\bar{M}_W$ (kDa)	d ($\bar{M}_W/\bar{M}_n$)	R_H (nm)	R_g (nm)	c* (mg/mL)
90	1.3	31	24	10.9
1100	1.2	112	87	2.8
1800	1.3	158	122	1.6
4000	1.2	291	225	0.6

Table 2. Rheological properties of HA solutions (G_0, η_0* and η_∞*) and network parameters (ν, M_c and ξ) for different $\bar{M}_W$ and concentrations.

$\bar{M}_W$ (kDa)	HA concentration (mg/mL)	G_0 (Pa)	η^*_0 (Pa s)	$\eta^*_\infty \cdot 10^4$ (Pa s)	$\nu \cdot 10^9$ (mol/mL)	$\bar{M}_c$ (kDa)	ξ (nm)
1100	5	5	0.1	5	2.0	384	625
	7.5	27	0.2	18	11.2	271	486
	10	81	0.9	54	33.2	182	386
	15	211	2.6	68	86.4	126	299
	20	308	5.1	220	126	117	265
1800	5	29	0.3	7	11.9	261	549
	7.5	57	1.5	36	23.3	220	453
	10	126	5.0	184	51.6	151	363
	15	271	26.0	337	111	113	288
	20	457	63.0	341	188	92	245
4000	5	43	10.6	180	17.7	242	535
	7.5	132	45.2	190	54.0	128	378
	10	290	117.4	220	119	80	294